Pediatric Radiology (2020) 50:1839–1854
https://doi.org/10.1007/s00247-020-04806-x

FETAL IMAGING

Fetal ultrasound and magnetic resonance imaging: a primer on how to interpret prenatal lung lesions

Niamh C. Adams[1] · Teresa Victoria[1] · Edward R. Oliver[1] · Julie S. Moldenhauer[2] · N. Scott Adzick[2] · Gabrielle C. Colleran[3,4]

Received: 20 March 2020 / Revised: 1 May 2020 / Accepted: 10 August 2020 / Published online: 19 November 2020

Abstract

Fetal lung lesions include common lesions such as congenital pulmonary airway malformation (CPAM), bronchopulmonary sequestration (BPS) and combined CPAM–BPS hybrid lesions, as well as less common entities including congenital lobar emphysema/obstruction, bronchial atresia, bronchogenic cysts and rare malignant pulmonary lesions such as pleuropulmonary blastoma. Fetal lung lesions occur in approximately 1 in 15,000 live births and are thought to arise from a spectrum of abnormalities related to airway obstruction and malformation, with the lesion type depending on the timing of insult, level of bronchial tree involvement, and severity of obstruction. Lesions vary from small and asymptomatic to large and symptomatic with significant mass effect on surrounding structures. Accurate diagnosis and characterization of these anomalies is crucial for guiding patient counseling as well as perinatal and postnatal management. The goal of this review is to provide an overview of normal fetal lung appearance and imaging features of common and uncommon lesions on both ultrasound and MR imaging, and to discuss key aspects in reporting and evaluating the severity of these lesions.

Keywords Congenital · Fetus · Lung · Magnetic resonance imaging · Neonate · Ultrasound

Introduction

Fetal lung lesions include common offenders such as congenital pulmonary airway malformation (CPAM), bronchopulmonary sequestration (BPS) and combined CPAM–BPS hybrid lesions, as well as less common entities including congenital lobar emphysema/overinflation (CLE/CLO), bronchial atresia, bronchogenic cysts, and rare malignant pulmonary lesions such as pleuropulmonary blastoma [1]. Important mimics that can erroneously be referred as pulmonary lesions include congenital high airway obstruction syndrome (CHAOS), mediastinal teratomas, lymphatic malformations, and sometimes congenital diaphragmatic hernia if the herniated intrathoracic liver is mistaken for a lung lesion. Fetal lung lesions occur in approximately 1 in 15,000 live births [2]. Congenital bronchopulmonary malformations such as CPAM, BPS, bronchial atresia and CLO are thought to arise from a spectrum of abnormalities related to airway obstruction and malformation, with the lesion type depending on the timing of insult, level of bronchial tree involvement, and severity of obstruction [3]. A number of lesions have a similar prenatal imaging appearance, and pathological diagnosis remains the gold standard for final diagnosis.

Lesions vary from small and asymptomatic to large and symptomatic with significant mass effect on surrounding structures. Accurate diagnosis and characterization of these anomalies is crucial for guiding patient counseling as well as perinatal and postnatal management. Treatment options for large masses include maternal administration of steroids, thoracentesis, thoracoamniotic shunts, open fetal surgical resection and postnatal surgical resection [4, 5]. A primary goal of imaging is to identify cases that require prenatal treatment or intervention and those that require additional perinatal planning and support.

✉ Niamh C. Adams
adamsn@tcd.ie

[1] Department of Radiology, Children's Hospital of Pennsylvania, 3401 Civic Center Blvd., Philadelphia, PA 19104, USA

[2] Department of Surgery, Children's Hospital of Pennsylvania, Philadelphia, PA, USA

[3] Department of Radiology, National Maternity Hospital, Dublin, Ireland

[4] Department of Radiology, Children's Health Ireland at Temple Street, Dublin, Ireland

Ultrasound (US) is the gold standard in imaging of the fetal lung. Ultrasound is widely available, relatively low in cost, well tolerated by patients and considered safe at all gestations. Congenital lung lesions are usually first identified at the time of the second-trimester anatomy scan. In experienced hands, detailed high-resolution US with Doppler assessment often allows for accurate prenatal diagnosis. Rapid-acquisition MRI has evolved as an essential complementary imaging modality to US in investigating fetal lung lesions because MRI often provides added diagnostic and prognostic information. It is particularly useful in equivocal or complex cases on US as well as in cases being considered for fetal treatment or intervention because of large size or complications. In these cases, MRI can provide better visualization of the lesion as well as the ipsilateral lung and contralateral lung, especially when there are technical difficulties with US because of patient size, fetal position or oligohydramnios.

Advantages of fetal MRI in general include multiplanar capability, large field of view and excellent contrast between bowel, lung and lung mass. Last, fetal MRI can provide diagnostic and prognostic information by allowing the calculation of fetal lung volumes.

In this review we provide an overview of normal fetal lung appearance and imaging features of common and uncommon lesions and discuss key aspects of reporting and evaluating the severity of these lesions.

Normal fetal lung appearance

Ultrasound

The fetal lung parenchyma demonstrates homogeneous echotexture throughout gestation (Fig. 1). In early pregnancy, normal lung is hypoechoic compared to liver parenchyma. With advancing gestational age, the lungs become more fluid-filled and progressively more echogenic relative to liver and muscle [6]. When visualized, the fetal airway is fluid-filled and hypoechoic on US. The diaphragm is hypoechoic compared to the adjacent lung parenchyma.

Magnetic resonance imaging

Fluid-sensitive sequences are the optimal sequences for evaluating lung anatomy (Fig. 2). The lungs typically contain a significant amount of alveolar fluid and are homogeneously hyperintense relative to the liver, spleen and chest wall musculature. Normal fetal lung signal intensity increases from 24 weeks of gestation because of the presence of increased fluid in the developing alveoli. This can be assessed by comparing the brightness of the lungs to surrounding structures including the liver, spleen, muscle and amniotic fluid [7]. Administration of steroids can result in increased lung parenchymal signal intensity on fluid-sensitive sequences. On T1-weighted imaging, the lungs are hypointense compared to liver, spleen and meconium.

The fetal airways, trachea and bronchi are T2-hyperintense fluid-filled structures. The thymus has intermediate signal intensity on T2-weighted sequences.

Imaging technique

Ultrasound

Complete US assessment includes a full gray-scale assessment of both lungs in three planes as well as evaluation for mass effect on surrounding structures. Fetal Doppler ultrasound is a crucial component of the examination, especially in the presence of a lung mass, to look for the arterial supply and venous drainage.

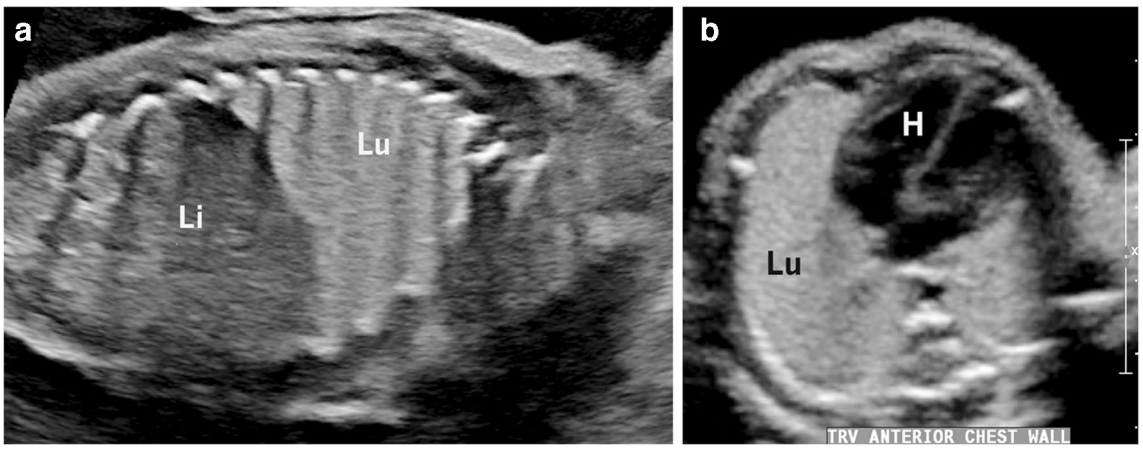

Fig. 1 Normal sonographic fetal lung signal. **a, b** Sagittal (**a**) and axial (**b**) sonographic views of a 25-week fetus demonstrate normal homogeneously echogenic lung (*Lu*) with respect to liver (*Li*) and heart (*H*)

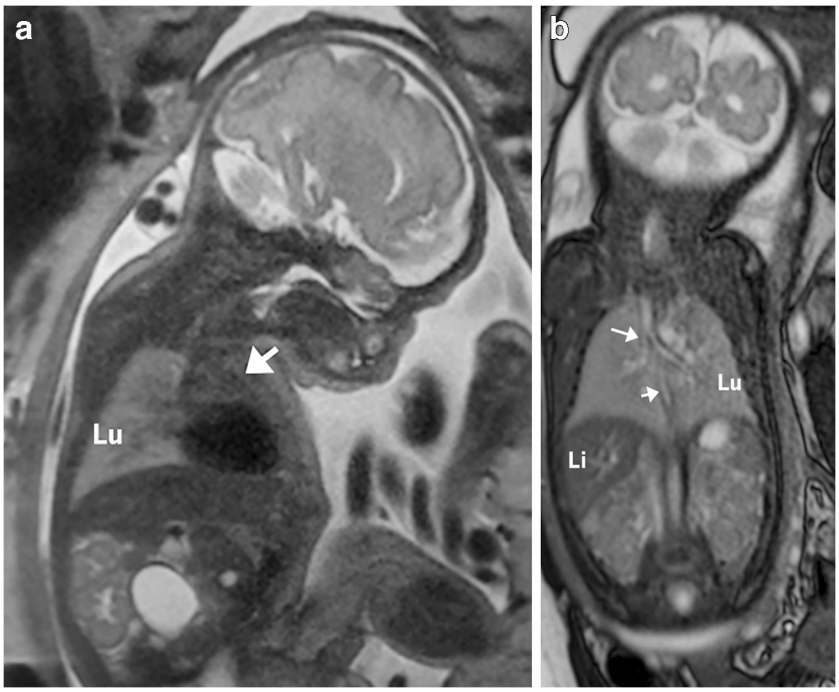

Fig. 2 Normal MR lung signal. **a, b** Sagittal single-shot fast spin-echo (SSFSE) (**a**) and coronal steady-state free precession (SSFP) (**b**) MR images in a 32-week fetus demonstrate a homogeneous lung parenchyma despite the relatively advanced gestational age. Note the airway and carina (*long arrow* in **b**) and esophagus (*short arrow* in **b**) as well as thymus (*arrow* in **a**). *Li* liver, *Lu* lung

The CPAM volume ratio (CVR) is a reliable method to express the size of a congenital lung lesion [8]. Lesion volume (mL) is first calculated using the formula of a prolate ellipsoid (height [cm] × width [cm] × length [cm] × 0.52) and then divided by the head circumference (cm). The CVR not only allows for lesions to be followed through gestation as the fetus grows, but it also provides important prognostic information because CVR values greater than 1.6 are associated with increased risk of developing hydrops. The CVR, therefore, can help in selecting which cases require close surveillance and possible in utero intervention [8].

Magnetic resonance imaging

Fluid-sensitive sequences are the preferred MR imaging modality for evaluating lung anatomy and characterizing masses. Standard MR imaging sequences include ultrafast sequences such as half-Fourier single-shot turbo spin-echo (SSTSE), free induction steady-state free precession sequences (SSFP), T1-weighted fast low-angle shot (FLASH) and echoplanar imaging (EPI). Diffusion-weighted imaging is also performed in select cases. Most fetal MRI examinations are performed on 1.5-tesla (T) magnets; however, the use of 3-T magnets is increasing because the higher magnet strength improves signal-to-noise ratio and allows for better evaluation of fetal anatomy [9].

Magnetic resonance imaging is particularly valuable in calculating fetal lung volumes because its superb tissue contrast helps distinguish the fetal lungs from adjacent structures. Briefly, the areas of the right and left lung volumes are individually calculated and added. Multiplying the total area by the sequence slice thickness (without gaps) provides the total lung volume. The observed total lung volume is then compared with the expected lung volume using reference standards for the given gestational age to give an observed over expected ratio [10, 11]. One of these reference standards was recently published, the result of a retrospective analysis of 665 patients who underwent fetal MRI for fetal lung volumes weekly from 18 weeks to 38 weeks [12]. At our institutions, we now use this as the reference standard; however, we continue to use the previously available reference standards for comparison (Rypens et al. [13] for fetuses ≥21 weeks). Meyers et al. [12] reinforces the method used by Rypens et al. [13] but provides more accurate total fetal lung volume measurements in the early second trimester as a result of Meyers's larger study population. An alternative way to measure lung volumes is by calculating them on a 3-D workstation. This is achieved by using a freehand tracing tool to trace the normal lung and its accompanying software to generate a 3-D volume measurement.

Evaluation of fetal lung maturation is also being investigated on fetal MRI. Areas of research include measuring T1 and T2 signal in the lungs relative to adjacent organs, e.g., liver and spleen at different gestational ages, and measuring apparent diffusion coefficient (ADC) values at different gestational ages. In a study by Yamoto et al. [14], the authors demonstrated in 88 control patients a correlation between increasing lung-to-liver signal intensity ratio and increasing gestation. Correlation between ADC values and gestational age was also shown in a series of 93 patients with normal lungs and 14 patients with congenital diaphragmatic hernia [15]. Further research to establish normative values for signal at different

gestational ages might provide additional prognostic information.

Virtual bronchoscopy has been attempted in fetal MRI by Werner et al. [16, 17]. This involves creating and evaluating 3-D representations of the bronchial tree from source images on MRI. This requires further investigation but has potentially useful clinical application for evaluating the fetal airway. For example, in a series of four fetuses with neck masses, this method was used to evaluate compression of the airway [17].

Lung lesions

Congenital pulmonary airway malformations

Congenital pulmonary airway malformations (CPAMs) are the most common fetal lung lesion, accounting for 30–50% of lesions, yet they are overall rare, complicating 1 in 25,000–35,000 pregnancies [18]. These lesions represent hamartomas of the lung and are characterized by abnormal branching of immature bronchioles, without normal alveolar development. They typically communicate with the normal tracheobronchial tree, although the communication is abnormal [1, 19]. These lesions have blood supply from the pulmonary arterial system and venous drainage to the pulmonary circulation. CPAMs are typically unilobar (85–95%), with the lower lobes being most commonly affected and without predilection for either lung [14].

Stocker et al. [20] first described a postnatal CPAM classification system of three types — Type I, Type II and Type III — and later added two further subclassifications, Type 0 and Type IV [21]. Type I consists of single or multiple large cysts (3–10 cm in diameter). Type I is the most common, accounting for 50–70% of cases. Type II CPAM contains various smaller cysts (0.5–2.0 cm). Type III consists of small cystic lesions that are rarely larger than 0.2 cm in diameter [22]; CPAM Type 0 is a solid-appearing lesion that consists almost exclusively of tracheal- and bronchial-like structures [23]. CPAM Type IV is characterized by peripheral thin-walled, often multiloculated cysts [24]. Adzick et al. [25] categorized prenatal CPAMs into two categories — macrocystic (multiple large cysts >5 mm) and microcystic (cysts measuring <5 mm) — to help guide perinatal management decisions.

The prenatal imaging appearance varies depending on the type of CPAM, but overall they are hyperechoic with respect to normal lung on US and T2 hyperintense on MRI, with focal cystic components being anechoic or T2 hyperintense (Figs. 3 and 4). Microcystic CPAMs often appear as a homogeneously solid hyperintense lesions on MRI and homogeneously hyperechoic on US. As the lungs become more hyperechoic/hyperintense with increasing gestational age, the conspicuity of lesions compared with the surrounding normal lung can decrease. Rarely, CPAM has solid T2-hypointense areas that correspond to areas of hypoechogenicity on US, an appearance that might represent an atypical, usually more focally aggressive CPAM (commonly fairly large in size and unresponsive to steroid administration) (Fig. 5), versus a congenital peribronchial myofibroblastic tumor [26].

The differential diagnosis for macrocystic CPAM includes hybrid lesions, pleuropulmonary blastoma and bronchogenic cysts. The differential diagnosis for microcystic CPAM includes BPS, hybrid lesions, CLO and bronchial atresia.

Maximum growth of a CPAM lesion typically occurs between 20 weeks and 26 weeks of gestation, with growth plateauing at 26–28 weeks [5]. In some cases, lesion size decreases during the late second trimester. In cases where the lesion appears to involute on prenatal imaging, postnatal imaging should still be performed because many of these neonates have a residual mass.

Bronchopulmonary sequestration

Bronchopulmonary sequestration (BPS) consists of abnormal pulmonary tissue that does not have a connection with the normal tracheobronchial tree and receives its arterial vascular supply from the systemic circulation. This systemic supply differentiates BPS from other congenital lung lesions. BPS accounts for up to 23% of prenatally detected lung lesions [27].

Bronchopulmonary sequestrations are classified as intralobar or extralobar. The intralobar subtype is typically enveloped within the normal visceral lung pleura and embedded within the normal lung parenchyma. The extralobar subtype can be supradiaphragmatic, subdiaphragmatic or transdiaphragmatic in location and has its own pleural lining [28].

The lower lobes, especially the left lower lobe, are the most common site for both subtypes. Venous drainage is typically to the pulmonary venous system in intralobar BPS and to the systemic veins, such as the inferior vena cava, portal veins and azygous vein, in extralobar sequestrations.

On imaging, BPS typically appears as homogeneous, solid, well-defined, hyperintense masses on T2-weighted MRI and solid hyperechoic lesions on US (Figs. 6, 7 and 8). Doppler US examination is useful in identifying the feeding vessels associated with BPS. A study by Oliver et al. [27] showed that US is most accurate for detecting systemic feeding arteries in bronchopulmonary sequestrations and hybrid lesions, and can also classify the lesions as intralobar or extralobar when draining veins are evaluated. Systemic arterial feeding vessels associated with BPS are not always identified on MRI. When the systemic feeding vessels are noted, they usually appear as low-signal linear structures in SSTSE images extending from the aorta into the BPS.

The differential diagnosis for intralobar BPS includes hybrid lesions as well as microcystic CPAM in fetuses where the feeding vessel is not seen on imaging. The differential diagnosis for an infradiaphragmatic extralobar BPS includes

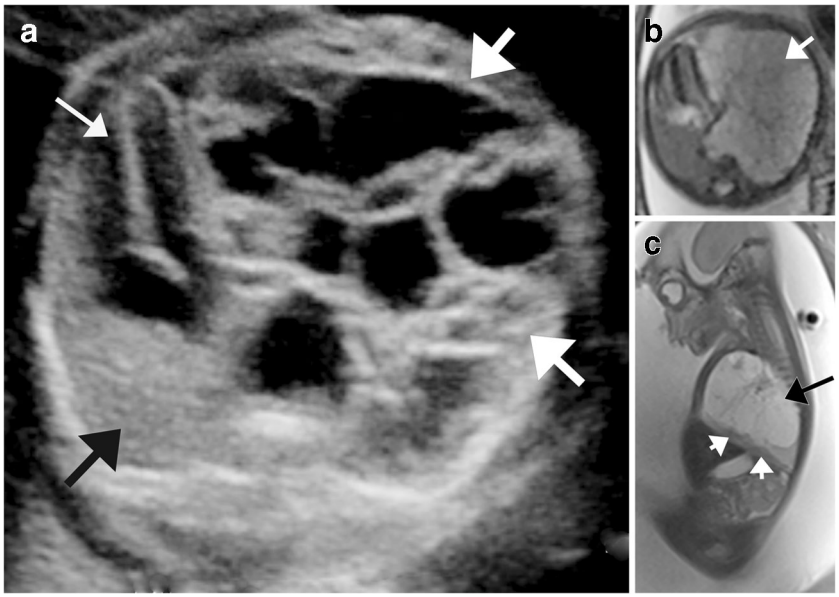

Fig. 3 Macrocystic congenital pulmonary airway malformation (CPAM). **a** Axial sonographic image of the chest in a 23-week fetus shows a CPAM in the upper lobe (*large white arrows*). Heart (*small white arrow*) and normal lung (*black arrow*) are denoted. Note significant mass effect of the lesion, which displaces the heart to the contralateral side. **b, c** Axial steady-state free precession (SSFP; **b**) and sagittal single-shot turbo spin-echo (SSTSE; **c**) MR images of the same fetus demonstrate the large macrocystic lesion (*large arrow*) with a small sliver of normal lung seen inferiorly in the sagittal view (*small arrows*)

neuroblastoma and adrenal hemorrhage, with neuroblastoma more likely to be diagnosed later in the third trimester [22].

Bronchopulmonary sequestration prognosis is usually favorable, and hydrops uncommonly occurs [29]. Prenatal management of BPS consists of careful observation. Although in utero resolution of BPS has been described, postnatal imaging with CT angiography is still indicated because usually a small residual lesion remains. Surgical excision of intralobar BPS is advisable because of the late risk of pulmonary infection or malignant transformation [30]. Asymptomatic extralobar BPSs without significant left-to-right shunting usually do not require resection. Timing of surgery depends on whether the lesion is symptomatic and how large the feeding artery is. A very large systemic arterial feeding vessel can cause high-output cardiac failure after birth because of the arteriovenous shunt through the extralobar BPS.

Congenital pulmonary airway malformation–bronchopulmonary sequestration hybrid lesions

Hybrid lesions are lesions that have features of both CPAM and BPS (Fig. 8) [31]. Hybrid lesions are common on imaging and even more so on pathological assessment, suggesting that the components have a common embryological origin. Appearances most commonly include a partially cystic lesion with systemic arterial supply and less commonly a solid lesion

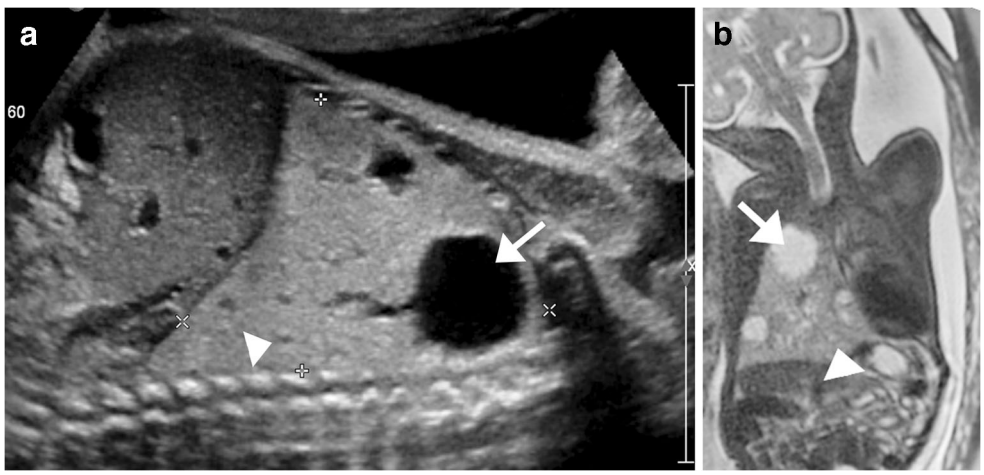

Fig. 4 Mixed macro- and microcystic congenital pulmonary airway malformation (CPAM). **a, b** Sagittal sonographic (**a**) and coronal single-shot turbo spin-echo (SSTSE) MR (**b**) images in a 30-week fetus show a large CPAM containing cysts measuring >5 mm (*arrows*) and <5 mm (*arrowheads*)

Fig. 5 Atypical congenital pulmonary airway malformation (CPAM) containing T2-hypointense elements. Coronal single-shot turbo spin-echo (SSTSE) MR image demonstrates a massive, predominantly solid atypical CPAM (*arrow*) occupying the entire left hemithorax and extending to the level of the lower abdomen in this 24-week fetus. The CPAM contains unusual T2-hypointense lesions, which at pathology correlated with unusually immature pulmonary elements. This type of CPAM might not regress following steroid administration

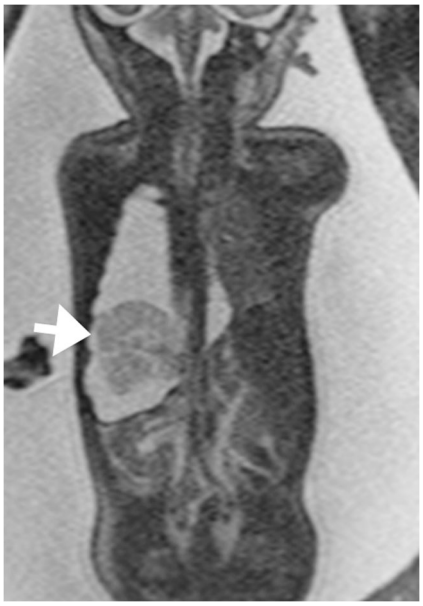

Fig. 7 Bronchopulmonary sequestration (BPS), extralobar. On coronal single-shot turbo spin echo (SSTSE) image, the extralobar sequestration (*arrow*) is surrounded by a large amount of pleural fluid in this 26-week fetus. In this case the vascular pedicle is very narrow, which can lead to vascular congestion and lymphatic overflow, as denoted by the nutmeg lung pattern of the lesion depicting the enlarged lymphatic vessels. Venous drainage was to the hemiazygous vein

with both systemic and pulmonary arterial supply. The presence of anomalous systemic arterial supply is essential for the diagnosis of a BPS/hybrid lesion. On pathology, characteristic features of congenital pulmonary airway malformations are present, with terminal respiratory bronchiolar overgrowth and cysts ranging in size from less than 1 mm to greater than 10 cm. As with bronchopulmonary sequestrations, hybrid lesions can be further classified as intralobar or extralobar based on their pleural investment and venous drainage. Typically, hybrid lesions have a better prognosis compared with CPAM lesions.

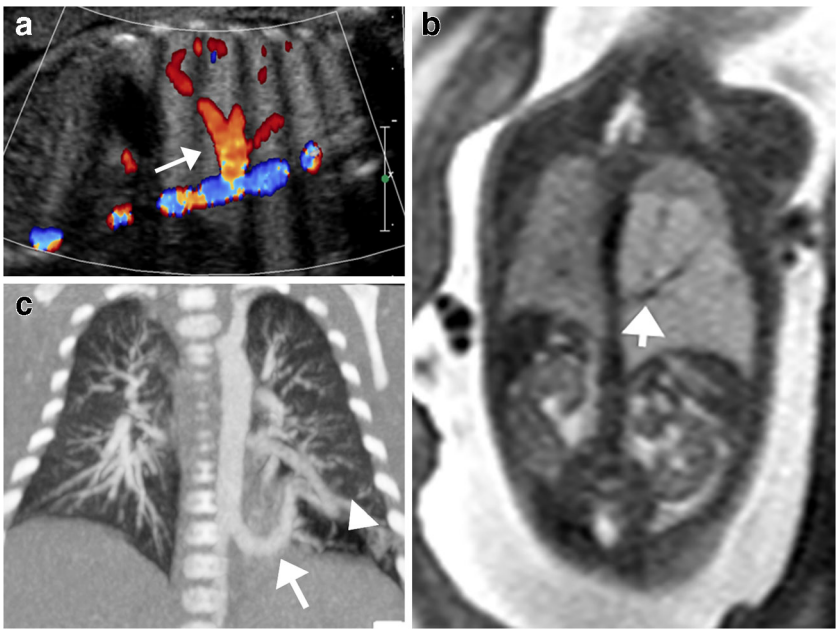

Fig. 6 Bronchopulmonary sequestration (BPS), intralobar. **a** Sagittal sonographic view of a left lower-lobe BPS shows an echogenic solid mass with a large feeding vessel (*arrow*) from the aorta in this 24-week fetus. **b** On coronal single-shot turbo spin-echo (SSTSE) MR image, the lesion is T2 hyperintense and the feeder is well seen in this black-blood sequence (*arrow*). **c** Postnatal coronal CT image demonstrates a partially aerated mass (*arrowhead*) with a large feeder from the thoracic aorta (*arrow*) in this intralobar BPS

Fig. 8 Hybrid lung lesion. Coronal single-shot turbo spin-echo (SSTSE) MR image denotes a hybrid lesion in a 27-week fetus. The T2-hyperintense lesion has components of sequestration (feeding vessel, *arrow*) and congenital pulmonary airway malformation (cyst, *arrowhead*)

Congenital lobar overinflation

Congenital lobar overinflation (CLO), also known as congenital lobar emphysema, results from bronchial obstruction, which can occur from an intrinsic airway abnormality (e.g., dysplastic bronchial cartilage) or from extrinsic compression of the airway by an adjacent structure (e.g., bronchogenic cyst). CLO is characterized by an area of lobar hyperdistension with normal pulmonary vascular supply and without the presence of macroscopic or microscopic cysts. After birth the bronchial obstruction produces a one-way valve effect with progressive distal air-trapping and frequent resultant respiratory distress.

Congenital lobar overinflation is a relatively rare pulmonary abnormality. The most common location is the apical and posterior segments of the left upper lobe, followed by the right middle lobe, right upper lobe, and much less commonly the lower lobes [32]. It is typically unilobar and rarely involves more than one lobe. A second less common form of CLO has been reported in association with bronchial atresia. In contrast to the more classic form of CLO, predisposition for lower-lobe involvement has been reported [33].

On second-trimester US, the typical appearance is of an echogenic, homogeneous, hyperechogenic mass without visible cysts (Fig. 9). The increased echogenicity of CLO is believed to be secondary to an abnormal accumulation of fluid in the involved lung. On third-trimester US exam the mass often becomes isoechoic to adjacent normal lung as the normal lung echogenicity increases and can be difficult to visualize. Mass effect might be the only clue that a CLO is present on prenatal US. A color Doppler finding in CLO is exuberant vascularity, with vascular flow identified to the periphery of the lesion at high pulse repetition frequencies (≥1,500 Hz). MR imaging shows a homogeneously hyperintense lesion on T2-W images. Stretching or elongation of nondisplaced hilar vessels has also been described on MRI [33, 34].

Bronchial atresia

Bronchial atresia is characterized by a focal obliteration of a bronchus with normal architecture of the distal lung. The airway obstruction prevents elimination of the distally produced pulmonary fluid, leading to fluid accumulation and expansion of the peripheral lung. The affected lung demonstrates homogeneous hyperechogenicity on US and hyperintensity on T2-weighted MR images [35] (Figs. 10 and 11).

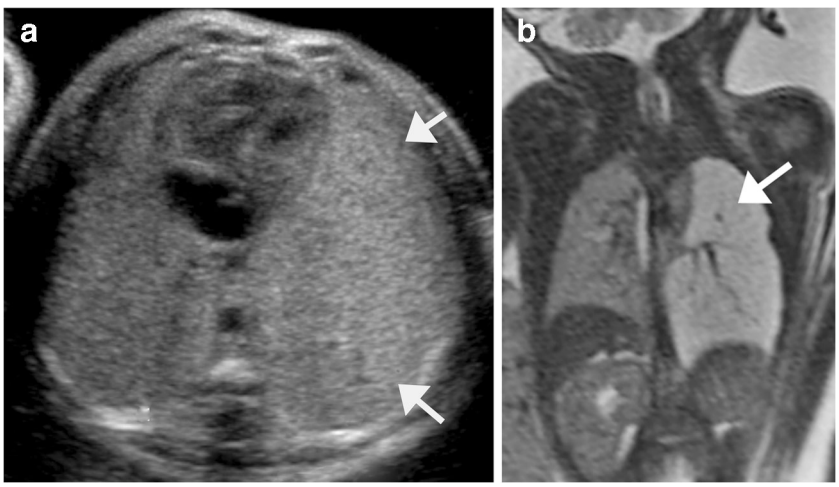

Fig. 9 Congenital lobar overinflation (CLO) in a 29-week fetus. **a** On transverse US image, the left-side CLO (*arrows*) is mildly hyperechoic compared to the contralateral normal right lung. **b** On coronal single-shot turbo spin-echo (SSTSE) MR image, the lesion is homogeneously hyperintense (*arrow*), without cysts or bronchial elements

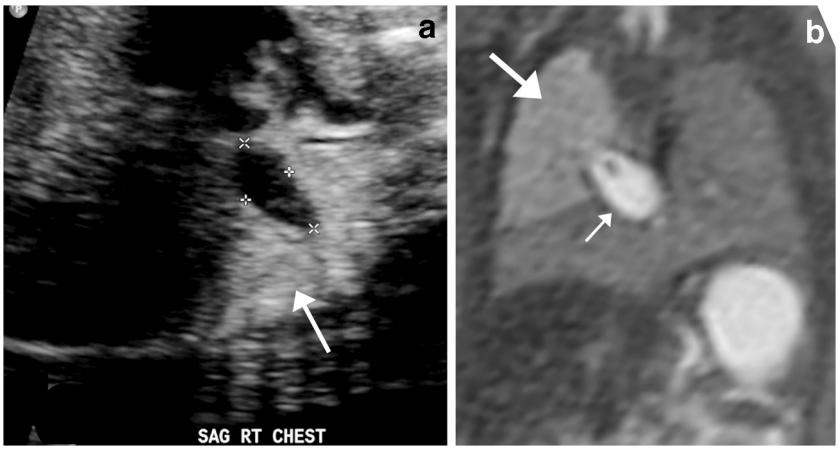

Fig. 10 Bronchial atresia. **a, b** Sagittal sonographic (**a**) and coronal single-shot turbo spin-echo (SSTSE) MR (**b**) images in a 24-week fetus with right upper lobe bronchial atresia (*arrow* in **a**, *large arrow* in **b**). The lesion has a centrally obstructing bronchocele, which is anechoic on US image (*calipers* in **a**) and T2 hyperintense on MR image (*small arrow* in **b**)

When bronchial atresia affects the proximal bronchi (e.g., mainstem or proximal lobar bronchus), the volume of the affected lung increases and becomes homogeneously hyperechogenic on US and T2 hyperintense on MR imaging relative to the normal lung, with associated mass effect on the ipsilateral diaphragm and mediastinum, and compression of contralateral lung. Fluid-filled tubular structures distal to the atresia might be seen as fluid/mucous accumulates in the proximal bronchi (bronchoceles). The right lung is more commonly affected in proximal atresias [35]. Central bronchial atresia has a very poor prognosis from hydrops and severe lung hypoplasia on the contralateral side.

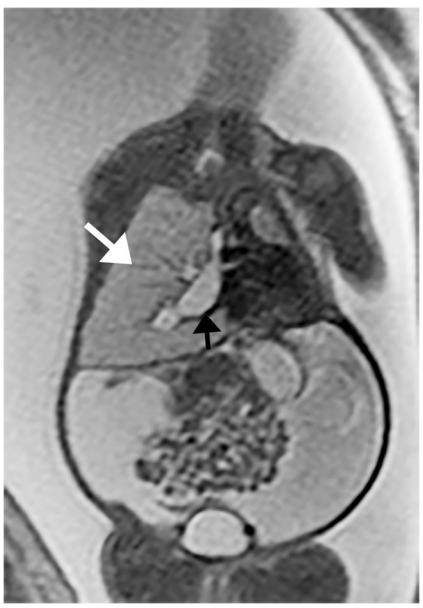

Fig. 11 Bronchial atresia. Coronal single-shot turbo spin-echo (SSTSE) MR image demonstrates a central bronchial atresia in a 26-week fetus manifested by obstruction and dilatation of the bronchi centrally (*black arrow*) and retained, hyperintense fluid distally (*white arrow*). The contralateral lung is markedly hypoplastic. The fetus is starting to demonstrate stress manifested by the large amount of ascites. There is no frank hydrops

More peripheral cases of bronchial atresia located at the segmental/subsegmental bronchial level present as an isolated lesion or in conjunction with other lesions, most commonly microcystic CPAM [36]. The locations most frequently involved are the apical and posterior segments of the left upper lobe. Imaging features include expansion of the associated segment with homogeneous hyperechogenicity on US images and hyperintensity on T2-weighted MR images relative to the normal lung. Bronchial dilation in central atresias can also be present in peripheral bronchial atresias.

Bronchogenic cyst

Bronchogenic cysts are fluid- and mucin-filled, blind-ending respiratory epithelial-lined pouches caused by abnormal budding from the ventral foregut along the tracheobronchial tree. Bronchogenic cysts account for 20–30% of congenital bronchopulmonary foregut cystic malformations [37]. They are typically unilocular. The majority of bronchogenic cysts originate in the region of the carina; however, 15% are intraparenchymal and therefore the differential diagnosis includes a CPAM with a single macrocyst [28] or pleuropulmonary blastoma. Less commonly, cysts arise from the pleura or diaphragm. Bronchogenic cysts are typically anechoic on US and T2 hyperintense on MRI. Internal signal on T1-weighted imaging is variable and depends on the proteinaceous content of the cyst (Figs. 12 and 13).

Congenital lung tumors

The vast majority of fetal lung masses are developmental anomalies, although very rarely congenital primary lung tumors are identified. These include congenital infantile fibrosarcoma/congenital peribronchial myofibroblastic tumor (CPMT), fetal lung interstitial tumor (FLIT) and pleuropulmonary blastoma. Neoplastic fetal lung masses can continue to grow late in gestation and lead to the development of hydrops during the third trimester. These might be

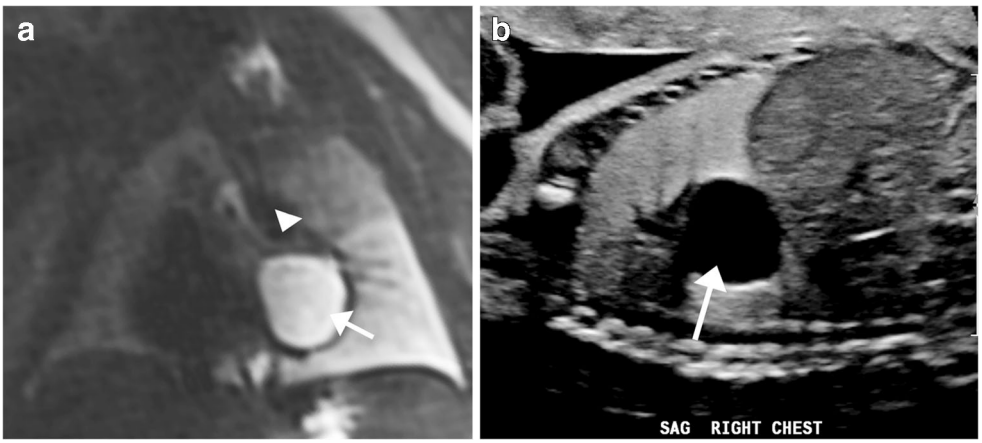

Fig. 12 Bronchogenic cyst. **a, b** Coronal single-shot turbo spin-echo (SSTSE) MR (**a**) and sagittal US (**b**) images in this 36-week fetus with a bronchogenic cyst (*arrows*) show regional mass effect onto the left bronchus (*arrowhead*) impeding the egress of fluid from the left lung, resulting in a hyperintense distal lung secondary to retained fluid

suspected when a rapidly enlarging mass is detected, usually at a late gestational age. They are typically well-circumscribed masses.

Congenital peribronchial myofibroblastic tumor

Previously thought to be a malignant tumor, CPMT is now recognized as a benign mass arising from embryonic pluripotent mesenchyme surrounding large developing bronchi. Given its pluripotent potential, the mass might contain different elements within it, including cartilage, smooth muscle elements and other potential histological cell types [38]. This is a rare tumor and might be suspected when there are heterogeneous echotexture on US and low signal foci on T1- and T2-weighted MR imaging indicative of fibrous tissue (Fig. 14). Note that this MR appearance is not exclusive of this type of tumor [26, 39]. The differential diagnosis includes atypical CPAM and congenital fibrosarcoma (described later in this paper). A differentiating feature is that this type of neoplasm is the only one that has been reported in the second trimester, to date [26, 40].

Pleuropulmonary blastoma

Pleuropulmonary blastoma (PPB) is a rare but aggressive tumor that presents during late gestation or early in infancy. The typical histopathological presentation includes the aggregation of malignant primitive small cells, usually observed in sheets [41]. It has been reported in 4% of lesions suspected to be CPAM prior to pathology [42]. PPB is a congenital malignancy and has been classified based on gross pathology into three types: Type 1 is cystic, Type 2 is solid and cystic, and Type 3 is predominantly solid. PPBs presenting in the prenatal period are usually Type 1. The imaging appearances reflect these subtypes (Fig. 14). It is usually difficult to differentiate PPB from other etiologies, especially CPAM, on prenatal imaging [43].

Fetal lung interstitial tumor

Fetal lung interstitial tumor (FLIT) was previously called "immature mesenchymal interstitial tumor of the lung." Histologically, the mass is characterized by interstitial lung

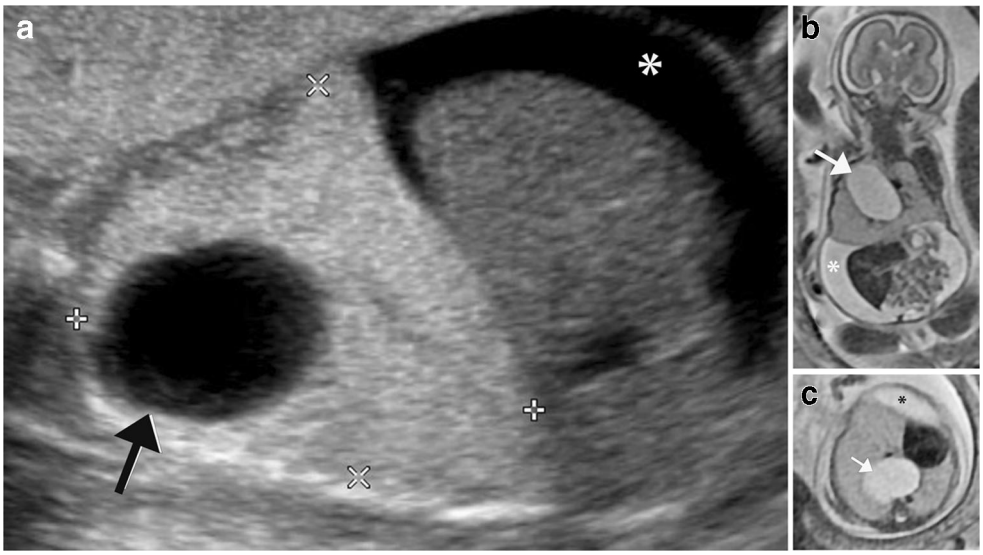

Fig. 13 Foregut duplication cyst in a 21-week fetus. **a–c** Sagittal ultrasound (**a**) and coronal (**b**) and axial (**c**) single-shot turbo spin-echo (SSTSE) MR images demonstrate an anechoic, T2-hyperintense cyst (*arrows*) obstructing the ipsilateral lung. There is subcutaneous edema and ascites (*asterisk*), compatible with hydrops. This patient had in utero cyst drainage and postnatal resection, with pathology compatible with an esophageal duplication cyst

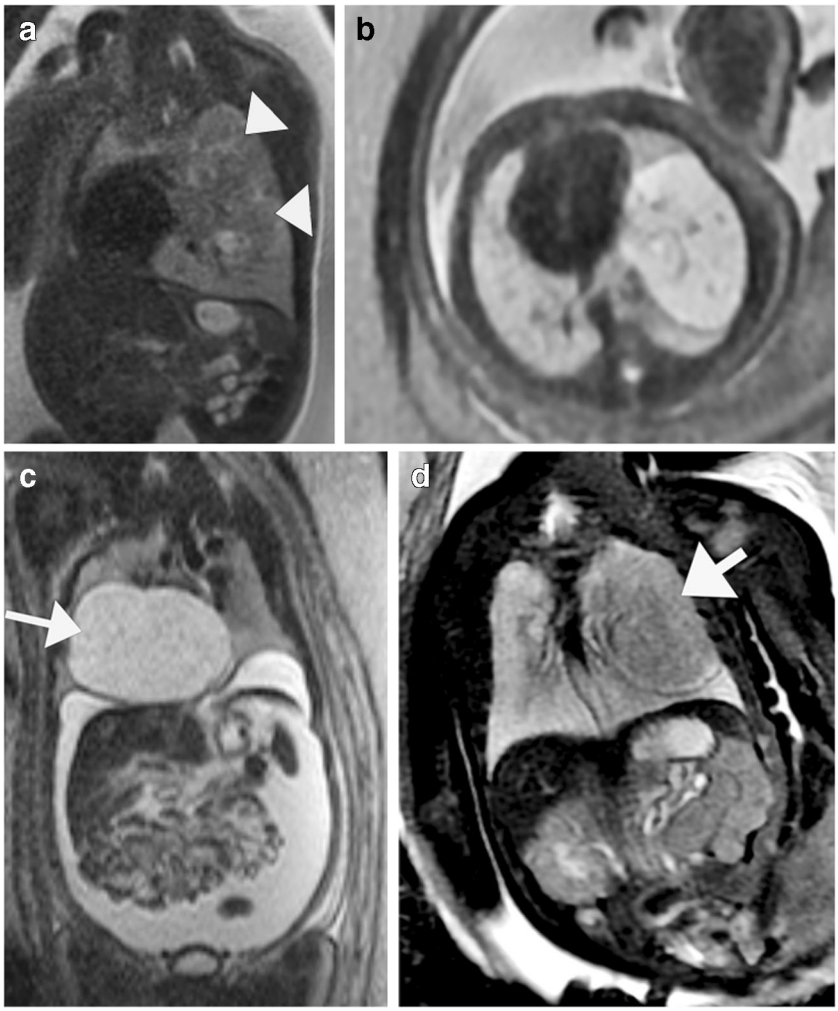

Fig. 14 Primary pulmonary tumors. **a** Congenital peribronchial myofibroblastic tumor (CPMT). Coronal single-shot turbo spin-echo (SSTSE) MR image in a 33-week fetus with a large mass (*arrowheads*) demonstrates predominantly T2-hypointense components, mixed with smaller cysts. On postnatal pathology the mass represented CPMT. **b** Pleuropulmonary blastoma (PPB). Axial SSTSE MR image shows a T2-hyperintense, well-marginated mass with no significant mass effect seen in the third-trimester (image courtesy of Beth Kline-Fath, MD). Note how PPB can be difficult to distinguish from a congenital pulmonary airway malformation (CPAM)-type lesion. **c** Fetal lung interstitial tumor (FLIT). Coronal SSTSE MR image in a 37-week fetus shows a large, solid, well-marginated T2-hyperintense mass (*arrow*) (image courtesy of Chris I. Cassady, MD). **d** Congenital fibrosarcoma. Coronal steady-state free precession MR image in a 36-week fetus shows an intrapulmonary T2-hypointense lesion (*arrow*) that pathology demonstrated to be a congenital fibrosarcoma (image courtesy of Erika Rubesova, MD)

cells that appear like fetal lung at 20–24 weeks of gestation [44]. FLIT is one of the most rare fetal lung masses, with only a few cases reported in the literature [45]. On US, FLIT demonstrates slightly increased echogenicity compared with normal lung. These tumors are well-circumscribed lesions. On MRI, FLIT appears as a solid mass that is hyperintense compared to liver and muscle. It can contain radiating bands of hyperintensity [45]. It appears very similar to microcystic CPAM and is usually diagnosed on pathology (Fig. 14).

Congenital pulmonary fibrosarcoma

A rare tumor seen prenatally, congenital pulmonary fibrosarcoma is a malignant spindle cell tumor that occurs most often in the soft tissues. When it involves the lungs, it usually involves the airway. Congenital pulmonary fibrosarcomas are highly cellular tumors made of cells arranged in interlacing fascicles or a herringbone pattern. Hemorrhage and necrosis might be present. As shown in Fig. 14, it should be included in the differential diagnosis of a T2-hypointense intrapulmonary mass.

Esophageal bronchus

Esophageal bronchi are a rare form of communicating bronchopulmonary foregut malformation and present in infancy with recurrent infection and a radiopaque hemithorax on chest radiography [46]. Until recently, they were only

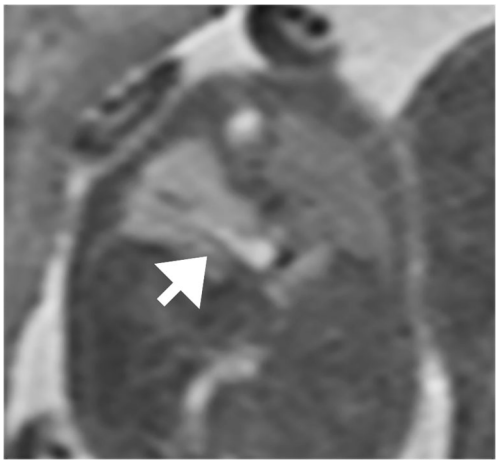

Fig. 15 Esophageal bronchus. Coronal single-shot turbo spin-echo (SSTSE) MR image in a 22-week fetus demonstrates a T2-hyperintense bronchocele (*arrow*) directed toward the stomach, rather than the bronchial tree, consistent with an esophageal bronchus

diagnosed postnatally, but a recent paper describes a tubular, anechoic and T2-hyperintense structure directed from a lung lesion to the gastroesophageal junction, which indicates the existence of such an entity [47]. It is important to know the existence of an esophageal bronchi to avoid the risk of aspiration pneumonitis secondary to feeding in the neonate. Esophageal bronchi have been associated with various lung lesions, predominantly BPS (Fig. 15).

Mimics of fetal lung lesions

Pleural effusion

The presence of fluid in the pleural space is considered an abnormal finding at all stages of gestation. This can have primary causes (e.g., lymphatic duct malformation) or can be secondary to immune or non-immune hydrops (Fig. 16). Pleural effusions are associated with additional pulmonary

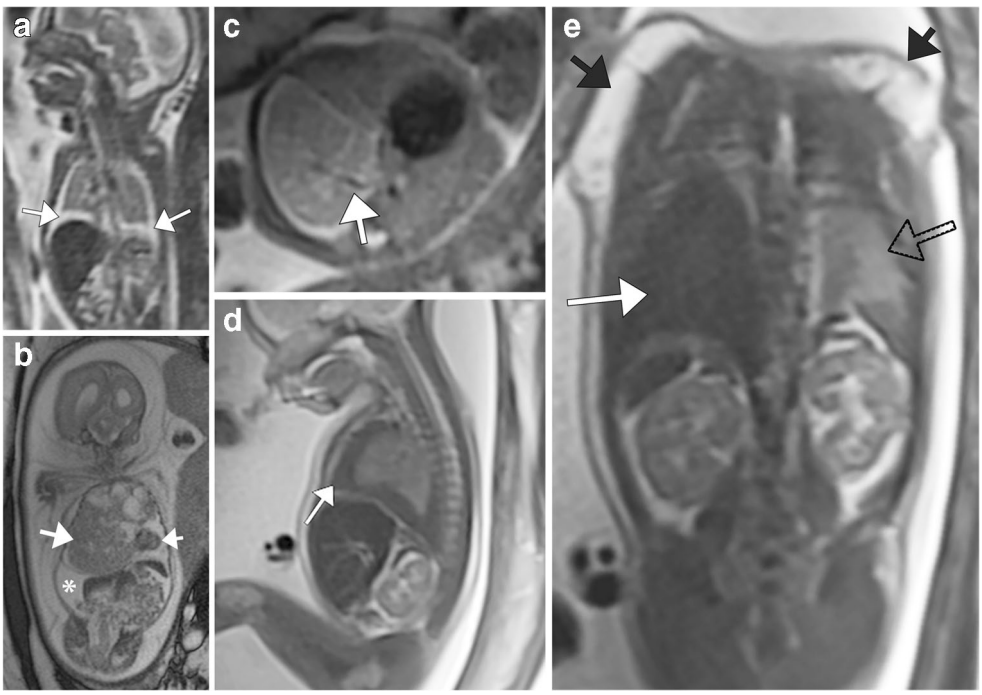

Fig. 16 Examples of fetal pleural effusions. **a** Coronal single-shot turbo spin-echo (SSTSE) MR image in an 18-week fetus shows bilateral pleural effusions (*arrows*) and contracted lungs. Collapsed lungs would usually have decreased T2 signal because of decreased fluid retention; these, however, have increased signal, a sign that might indicate a lymphatic abnormality. On postnatal MR lymphangiogram the infant was shown to lack the cisterna chyli and thoracic duct, and demonstrated diffuse abnormal lymphatic perfusion. **b** Coronal SSTSE MR image in a 20-week fetus shows a large mediastinal teratoma (*large arrow*) resulting in marked displacement of the heart (*small arrow*) and findings of hydrops manifested as bilateral pleural effusions, ascites (*asterisk*) and marked skin thickening. Oligohydramnios was also present. **c** Axial SSTSE MR image in a 20-week fetus shows extralobar sequestration (see feeder from thoracic aorta denoted by *arrow*). The mass has a heterogeneous appearance and is surrounded by T2-hyperintense simple pleural fluid. The heterogeneous appearance of the mass is thought to be from vascular/lymphatic congestion in extralobar bronchopulmonary sequestrations that have a narrow vascular pedicle. **d, e** Sagittal (**d**) and coronal (**e**) SSTSE MR images demonstrates an unusual T2-hypointense pleural effusion (*white arrows*) in this 24-week fetus with sandal toe deformity (not shown) and numerous posterior thoracic subcutaneous lymphatic malformations (*solid black arrows* in **e**). The pleural effusion was anechoic on US and T1 hypointense and resulted in a contracted lung (*empty black arrow* in **e**). The combination of lymphatic malformations and skeletal abnormalities, together with large size for gestational age, led to the diagnosis of CLOVES (congenital lipomatous overgrowth [CLO], vascular malformation [V], epidermal nevi [E] and scoliosis and spinal deformities [S])

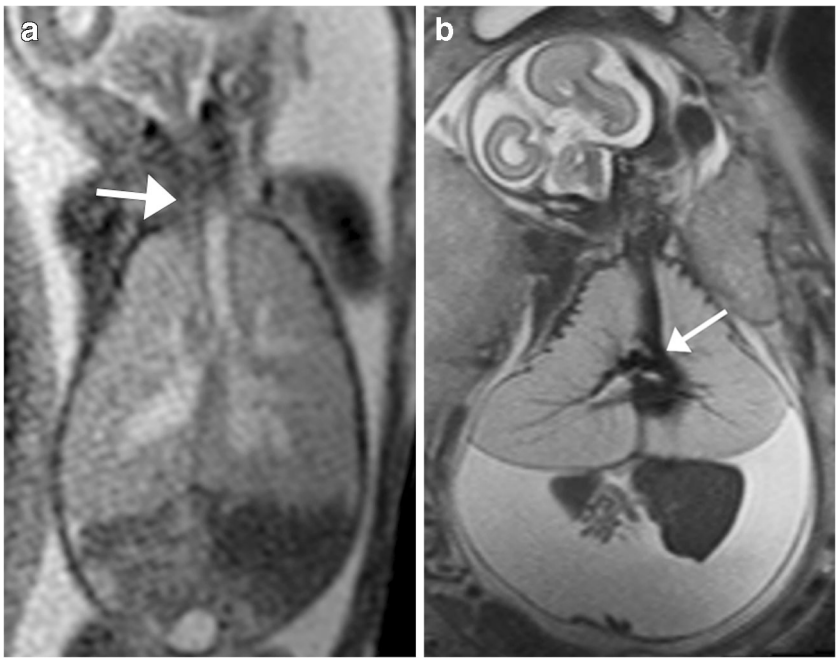

Fig. 17 Congenital high-airway obstruction syndrome (CHAOS). **a, b** Coronal steady-state free precession (SSFP) (**a**) and single-shot turbo spin-echo (SSTSE) (**b**) MR images in two fetuses with CHAOS, one with a high obstruction at the level of the larynx (*arrow* in **a**; 20-week fetus), the second with obstruction at the level of the carina (*arrow* in **b**; 21-week fetus). Defining the site of obstruction is a crucial job for the radiologist because this determines the accessibility of the airway and mode of delivery

and extrapulmonary abnormalities in approximately 40% of cases. Fetal US and MR images allow for the assessment of associated abnormalities. Simple pleural fluid is hyperintense on T2- and hypointense on T1-W imaging and surrounds lung in the pleural space. On US there is an anechoic region surrounding the fetal lung. If effusions are large they can cause lung compression and pulmonary hypoplasia, similar to other lung masses. It is important to evaluate for other signs of hydrops in the presence of a pleural effusion.

Congenital high-airway obstruction syndrome

Congenital high-airway obstruction syndrome (CHAOS) is characterized by complete or near-complete obstruction of the fetal airway leading to the trapping of lung fluids, hyperplasia of pulmonary alveoli, and airway dilatation. This can be caused by a number of conditions including atresia, stenosis or obstruction (web) at the level of the larynx, or supraglottic or subglottic trachea [48].

On US both lungs are significantly symmetrically enlarged and echogenic. The heart is centrally located and there is typically mass effect on the cardiac chambers and eversion of the diaphragm (Figs. 17 and 18).

MRI is helpful in identifying the precise level of airway obstruction for the treatment planning required for postnatal airway management. Fetal T2-weighted MRI shows enlarged hyperintense lungs with mass effect on the heart and diaphragm and might show a dilated airway. The diagnosis should be considered in cases where there are bilateral hyperintense lung lesions. Identifying the level of obstruction is crucial to imaging because it guides the possibility of postnatal treatment planning. Hydrops is a common complication caused by impaired venous return by the hyperinflated lungs [19].

Lymphatic malformation

Congenital lymphatic malformation is a hamartoma of the lymphatic system. Although they have benign histology they can grow rapidly and infiltrate locally into the muscle, bone and underlying tissue, leading to morbidity. They do not communicate with the normal lymphatic system. They occur in approximately 1 in 6,000 live births [49]. The most common location is in the neck; however, intrathoracic and mediastinal lymphatic malformations also occur and are in the differential diagnosis for cystic mass in the chest (Fig. 19). Although nuchal lymphatic malformations are associated with multiple conditions, intrathoracic lymphatic malformations are typically diagnosed later in gestation and have a low incidence of associated chromosomal and structural anomalies [50].

Intrathoracic lymphatic malformation typically presents as a uniseptate or multiseptate mass. On US these appear as multilocular cystic lesions, usually hypoechoic, with thin or thick hyperechoic septae. Vascular flow on color Doppler is typically absent. Fluid-fluid levels or mixed-echogenicity contents can be seen in cases of hemorrhage. On MRI, these lesions demonstrate multiple T2-hyperintense cystic locules with intervening septae. Some locules have T1-hyperintense hemorrhage within them or blood-fluid levels. Unilocular lymphatic malformations can occur but differ from pleural effusions because the fluid contents of lymphatic malformations appear contained and frequently exert localized mass effect, unlike in pleural effusions.

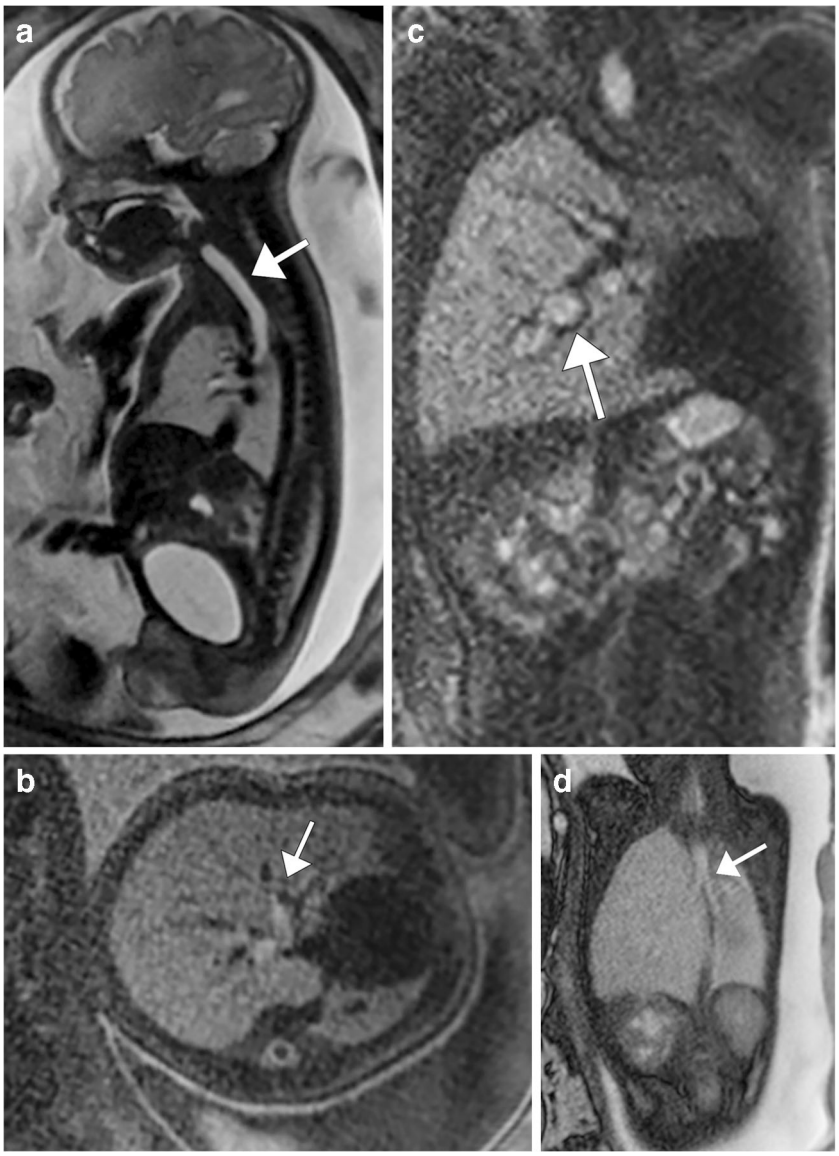

Fig. 18 Obstructive lesion: congenital high-airway obstruction syndrome (CHAOS) or not? **a–c** Sagittal (**a**), axial (**b**) and coronal (**c**) single-shot turbo spin-echo (SSTSE) MR images in a 32-week fetus show massive tracheomegaly (*arrow* in **a**) as well as distension of the right central bronchi (*arrows* in **b** and **c**). The degree of tracheal distension led to a prenatal diagnosis of subglottic obstruction. Interestingly, the left central bronchi was normal in caliber, although the left lung was hypoplastic. **d** Of note, a normal carina was present, as seen in this coronal steady-state free precession MR image (*arrow*). At immediate postnatal surgery, bronchoscopy demonstrated subglottic stenosis, tracheomegaly and dilated right central bronchi (and relatively normal left bronchi), with preferential hyperinflation of the right lung

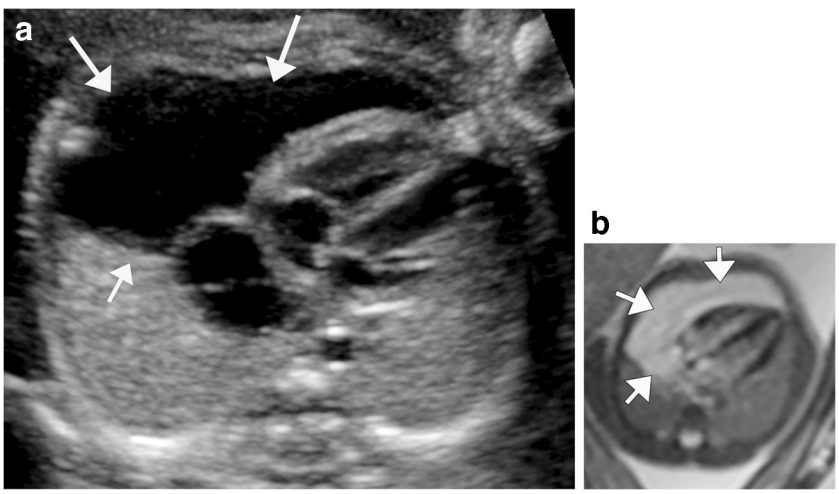

Fig. 19 Fetal lymphatic malformation. **a, b** US (**a**) and single-shot turbo spin-echo (SSTSE) MR (**b**) axial images in a 21-week fetus show a predominantly cystic lesion containing several internal, thin septations (*arrows*). On cine images, the lesion moved distinctly from the heart and the lung. The prenatal diagnosis was a lymphatic malformation, which was confirmed on postnatal imaging

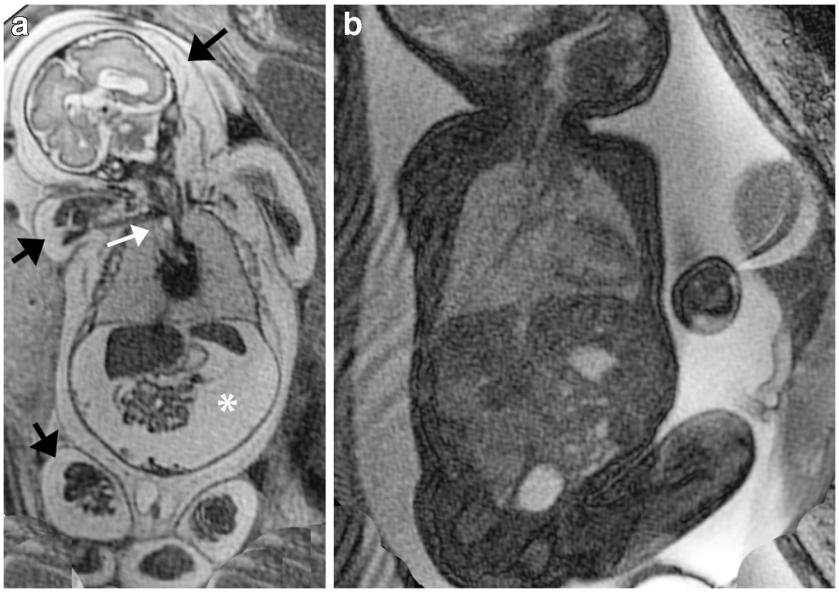

Fig. 20 Evaluation of global mass effect exerted by the lesion onto the fetus. **a** Coronal single-shot turbo spin-echo (SSTSE) MR image in a 32-week fetus shows findings of congenital high-airway obstruction syndrome (CHAOS) secondary to a small bronchogenic cyst (*white arrow*) arising from the trachea and restricting the egress of fluid. Note that the heart is midline but compressed, and the lungs are hyperintense and enlarged, with flattening of the diaphragms, secondary to the retained fluid. Ascites (*asterisk*) and diffuse skin thickening (*black arrows*) are seen, consistent with hydrops. Oligohydramnios was also noted. **b** Interestingly, at 38 weeks, the findings of hydrops resolved, including findings of ascites and skin thickening, as seen in this coronal steady-state free precession (SSFP) MR image. The small bronchogenic cyst was no longer identified, suggesting that it might have spontaneously decompressed, and amniotic fluid volume normalized. The infant was delivered via ex utero intrapartum treatment, with immediate bronchoscopy demonstrating the decompressed cyst. The neonate was discharged to home at 3 weeks of age on room air

Key imaging features that influence treatment decisions and prognosis: what the pediatric surgeon and maternal–fetal medicine physician want to know

When evaluating a fetal lung mass, a number of imaging findings help establish or narrow the diagnosis as well as guide management. For example, identification of systemic arterial supply suggests the diagnosis of BPS or hybrid lesion, whereas a solid lesion associated with a bronchocele suggests bronchial atresia.

Evaluating the size of the mass and lung volumes in the ipsilateral and contralateral lung is another crucial element of prenatal assessment. Pulmonary hypoplasia is characterized by underdevelopment and decreased numbers of alveoli and bronchi resulting in a decreased lung size and weight. Secondary pulmonary hypoplasia can be caused by any lesion that is large enough to compress the adjacent developing lung. The degree of lung hypoplasia/remaining lung volume is a key prognostic factor in fetal lung lesions and a crucial factor for treatment decisions. Marked reduction of signal intensities on MRI with decrease in lung echogenicity on US as well as decreased lung volumes are characteristic findings in fetuses with pulmonary hypoplasia.

The overall dimensions of the mass in three planes can be evaluated on US and MR imaging. As noted, the CVR is a crucial measurement in conveying lesion size: a CVR greater than 1.6 was found to be significant, with a 3- to 4-fold higher rate of hydrops, need for fetal intervention, and fetal or postnatal death [8]. Increase in volume ratio on serial US exams is also a concerning finding. This measurement can be repeated at every US assessment and allows the relative size of the mass to the growing fetus to be tracked. On MRI, the fetal MRI-derived lung–mass volume ratio and lesion-to-lung volume ratio can also be calculated.

For all lung lesions, especially large lesions, it is crucial to assess their impact on surrounding structures. It is important to look for flattening or eversion of the hemidiaphragm, cardiomediastinal shift, compression of the uninvolved ipsilateral lung lobes and compression of the contralateral lung (Fig. 20). Searching for these signs of mass effect and for signs of hydrops helps identify patients who require prenatal treatment, early delivery or immediate postnatal treatment.

Hydrops is defined as abnormal fluid in two or more fetal compartments, including the pleural space, pericardial space, peritoneal space and subcutaneous tissue. Placentomegaly can also occur but is not a component of hydrops. Hydrops results from right-side heart failure secondary to compression of venous return to the heart.

Amniotic fluid volume should also be assessed. Polyhydramnios can occur from compression of the esophagus and impairment of swallowing. This can predispose the gravid patient to early delivery.

Follow-up

The natural history of lung lesions typically demonstrates an increase in size during the canalicular phase of lung development, from about 18 weeks to 26 weeks of gestation. After 26 weeks, most lesions plateau and stop growing or decrease in size relative to the overall size of the fetus [2]. A number of lesions become occult; however, a small proportion of lesions also increase in size dramatically and can lead to compression of the surrounding structures, including mediastinum, vena cava and heart, causing impaired right atrial blood return and findings of fetal hydrops, heart failure and even fetal death unless treated.

All lung masses including small ones should be followed because some increase in size later than expected by typical natural history of lung lesions [2]. Typical surveillance follow-up intervals are 1–2 weeks, depending on lesion size, with higher-CVR lesions followed at a shorter interval to better assess the lesion's growth trajectory and need for possible intervention (e.g., maternal betamethasone administration or cyst drainage/shunt placement). A longer follow-up interval can be considered in cases where the lesion is very small and without mass effect. In all patients with prenatally detected lung malformations, postnatal chest CT angiogram including the upper abdomen should be performed, for two reasons: some lesions that appear to disappear on prenatal imaging are still present on postnatal CT angiography, and CT angiography can help in preparation of possible surgical resection.

Summary

Imaging plays an essential role in the workup of fetal lung lesions and guides treatment and patient counseling. While US is the gold standard, the complementary role of MRI is well established and is most valuable in the assessment of larger and more complex lesions.

Compliance with ethical standards

Conflicts of interest None

References

1. Epelman M, Kreiger PA, Servaes S et al (2010) Current imaging of prenatally diagnosed congenital lung lesions. Semin Ultrasound CT MR 31:141–157
2. Cass DL, Olutoye OO, Cassady CI et al (2011) Prenatal diagnosis and outcome of fetal lung masses. J Pediatr Surg 46:292–298
3. Kunisaki SM, Fauza DO, Nemes LP et al (2006) Bronchial atresia: the hidden pathology within a spectrum of prenatally diagnosed lung masses. J Pediatr Surg 41:61–65
4. Peranteau WH, Boelig MM, Khalek N et al (2016) Effect of single and multiple courses of maternal betamethasone on prenatal congenital lung lesion growth and fetal survival. J Pediatr Surg 51:28–32
5. Adzick NS (2009) Management of fetal lung lesions. Clin Perinatol 36:363–376
6. Bulas D, Egloff AM (2011) Fetal chest ultrasound and magnetic resonance imaging: recent advances and current clinical applications. Radiol Clin N Am 49:805–823
7. Kasprian G, Balassy C, Brugger PC, Prayer D (2006) MRI of normal and pathological fetal lung development. Eur J Radiol 57:261–270
8. Crombleholme TM, Coleman B, Hedrick H et al (2002) Cystic adenomatoid malformation volume ratio predicts outcome in prenatally diagnosed cystic adenomatoid malformation of the lung. J Pediatr Surg 37:331–338
9. Victoria T, Johnson AM, Edgar JC et al (2016) Comparison between 1.5-T and 3-T MRI for fetal imaging: is there an advantage to imaging with a higher field strength? AJR Am J Roentgenol 206: 195–201
10. Victoria T, Bebbington MW, Danzer E et al (2012) Use of magnetic resonance imaging in prenatal prognosis of the fetus with isolated left congenital diaphragmatic hernia. Prenat Diagn 32:715–723
11. Danzer E, Victoria T, Bebbington MW et al (2012) Fetal MRI-calculated total lung volumes in the prediction of short-term outcome in giant omphalocele: preliminary findings. Fetal Diagn Ther 31:248–253
12. Meyers ML, Garcia JR, Blough KL et al (2018) Fetal lung volumes by MRI: normal weekly values from 18 through 38 weeks' gestation. AJR Am J Roentgenol 211:432–438
13. Rypens F, Metens T, Rocourt N et al (2001) Fetal lung volume: estimation at MR imaging-initial results. Radiology 219:236–241
14. Yamoto M, Iwazaki T, Takeuchi K et al (2018) The fetal lung-to-liver signal intensity ratio on magnetic resonance imaging as a predictor of outcomes from isolated congenital diaphragmatic hernia. Pediatr Surg Int 34:161–168
15. Cannie M, Jani J, De Keyzer F et al (2009) Diffusion-weighted MRI in lungs of normal fetuses and those with congenital diaphragmatic hernia. Ultrasound Obstet Gynecol 34:678–686
16. Werner H, Dos Santos JR, Fontes R et al (2011) Virtual bronchoscopy in the fetus. Ultrasound Obstet Gynecol 37:113–115
17. Werner H, Lopes dos Santos JR, Fontes R et al (2013) Virtual bronchoscopy for evaluating cervical tumors of the fetus. Ultrasound Obstet Gynecol 41:90–94
18. Langston C (2003) New concepts in the pathology of congenital lung malformations. Semin Pediatr Surg 12:17–37
19. Barth RA (2012) Imaging of fetal chest masses. Pediatr Radiol 42: S62–S73
20. Stocker JT, Madewell JE, Drake RM (1977) Congenital pulmonary airway malformation — a new name for and an expanded classification of congenital cystic adenomatoid malformation of the lung. Classification and morphologic spectrum. Hum Pathol 8:155–171
21. Stocker JT, Dehner LP, Inc OT (2002) Pediatric pathology. Lippincott Williams & Wilkins, Philadelphia
22. Daltro P, Werner H, Gasparetto TD et al (2010) Congenital chest malformations: a multimodality approach with emphasis on fetal MR imaging. Radiographics 30:385–395
23. Stocker JT (2009) Cystic lung disease in infants and children. Fetal Pediatr Pathol 28:155–184
24. Annunziata F, Bush A, Borgia F et al (2019) Congenital lung malformations: unresolved issues and unanswered questions. Front Pediatr 7:239
25. Adzick NS, Harrison MR, Crombleholme TM et al (1998) Fetal lung lesions: management and outcome. Am J Obstet Gynecol 179: 884–889
26. Victoria T, Srinivasan AS, Pogoriler J et al (2018) The rare solid fetal lung lesion with T2-hypointense components: prenatal

imaging findings with postnatal pathological correlation. Pediatr Radiol 48:1556–1566
27. Oliver ER, DeBari SE, Giannone MM et al (2018) Going with the flow: an aid in detecting and differentiating bronchopulmonary sequestrations and hybrid lesions. J Ultrasound Med 37:371–383
28. Johnson AM, Hubbard AM (2004) Congenital anomalies of the fetal/neonatal chest. Semin Roentgenol 39:197–214
29. Riley JS, Urwin JW, Oliver ER et al (2018) Prenatal growth characteristics and pre/postnatal management of bronchopulmonary sequestrations. J Pediatr Surg 53:265–269
30. Newman B (2006) Congenital bronchopulmonary foregut malformations: concepts and controversies. Pediatr Radiol 36: 773–791
31. Cass DL, Crombleholme TM, Howell LJ et al (1997) Cystic lung lesions with systemic arterial blood supply: a hybrid of congenital cystic adenomatoid malformation and bronchopulmonary sequestration. J Pediatr Surg 32:986–990
32. Mani H, Suarez E, Stocker JT (2004) The morphologic spectrum of infantile lobar emphysema: a study of 33 cases. Paediatr Respir Rev 5:S313–S320
33. Seo T, Ando H, Kaneko K et al (2006) Two cases of prenatally diagnosed congenital lobar emphysema caused by lobar bronchial atresia. J Pediatr Surg 41:e17–e20
34. Oliver ER, DeBari SE, Horii SC et al (2019) Congenital lobar overinflation: a rare enigmatic lung lesion on prenatal ultrasound and magnetic resonance imaging. J Ultrasound Med 38:1229–1239
35. Alamo L, Reinberg O, Vial Y et al (2013) Comparison of foetal US and MRI in the characterisation of congenital lung anomalies. Eur J Radiol 82:e860–e866
36. Peranteau WH, Merchant AM, Hedrick HL et al (2008) Prenatal course and postnatal management of peripheral bronchial atresia: association with congenital cystic adenomatoid malformation of the lung. Fetal Diagn Ther 24:190–196
37. Parikh D, Samuel M (2005) Congenital cystic lung lesions: is surgical resection essential? Pediatr Pulmonol 40:533–537
38. Reiss A, Goldberg Y, Monichor M, Drugan A (2005) Congenital pulmonary myofibroblastic tumor — pathology and prenatal sonographic appearance. Prenat Diagn 25:1064–1066
39. Calvo-Garcia MA, Lim FY, Stanek J et al (2014) Congenital peribronchial myofibroblastic tumor: prenatal imaging clues to differentiate from other fetal chest lesions. Pediatr Radiol 44:479–483
40. Waelti SL, Garel L, Soglio DD et al (2017) Neonatal congenital lung tumors — the importance of mid-second-trimester ultrasound as a diagnostic clue. Pediatr Radiol 47:1766–1775
41. Zhang H, Xu CW, Wei JG et al (2015) Infant pleuropulmonary blastoma: report of a rare case and review of literature. Int J Clin Exp Pathol 8:13571–13577
42. Coleman A, Kline-Fath B, Stanek J, Lim FY (2016) Pleuropulmonary blastoma in a neonate diagnosed prenatally as congenital pulmonary airway malformation. Fetal Diagn Ther 39: 234–237
43. Miniati DN, Chintagumpala M, Langston C et al (2006) Prenatal presentation and outcome of children with pleuropulmonary blastoma. J Pediatr Surg 41:66–71
44. Dishop MK, McKay EM, Kreiger PA et al (2010) Fetal lung interstitial tumor (FLIT): a proposed newly recognized lung tumor of infancy to be differentiated from cystic pleuropulmonary blastoma and other developmental pulmonary lesions. Am J Surg Pathol 34: 1762–1772
45. Phillips J, Blask A, DiPoto BA et al (2019) Fetal lung interstitial tumor: prenatal presentation of a rare fetal malignancy. J Neonatal Perinatal Med 12:473–477
46. Colleran GC, Ryan CE, Lee EY et al (2017) Computed tomography and upper gastrointestinal series findings of esophageal bronchi in infants. Pediatr Radiol 47:154–160
47. Partridge EA, Victoria T, Coleman BG et al (2015) Prenatal diagnosis of esophageal bronchus — first report of a rare foregut malformation in utero. J Pediatr Surg 50:306–310
48. Mong A, Johnson AM, Kramer SS et al (2008) Congenital high airway obstruction syndrome: MR/US findings, effect on management, and outcome. Pediatr Radiol 38:1171–1179
49. Farnaghi S, Kothari A (2013) The value of early recognition of fetal lymphangioma. Australas J Ultrasound Med 16:147–152
50. Goldstein I, Leibovitz Z, Noi-Nizri M (2006) Prenatal diagnosis of fetal chest lymphangioma. J Ultrasound Med 25:1437–1440